JOURNAL
OF THE AMERICAN CHEMICAL SOCIETY

VOLUME 101, NUMBER 12 JUNE 6, 1979

Some Hydrido-Bridged Transition-Metal Dimers and Their Unsupported Analogues. Speculations on Pentuple Bonding and Pentuple Bridging

Alain Dedieu,[1a] Thomas A. Albright,*[1b] and Roald Hoffmann*[1c]

Contribution from the E.R. No. 139 du C.N.R.S., Universite Louis Pasteur, 67000 Strasbourg, France, the Department of Chemistry, University of Houston, Houston, Texas 77004, and the Department of Chemistry, Cornell University, Ithaca, New York 14853. *Received January 7, 1979*

Abstract: Bonding and rotational barriers in M_2L_6 and M_2L_8 dimers in several alternative geometries are described. These barriers in most cases are determined by electronic factors, although steric requirements may occasionally play a dominant role. The magnitudes of the barriers depend on the number of electrons in the system and the electronic nature of the ligands. The dimer levels are then used to construct molecular orbitals for hydrido-bridged species. The conformational preferences of $H_3M_2L_6$ and $H_4M_2L_8$ are compared to experiment and the possible existence of $H_5M_2L_6$ and $H_3M_2L_8$ (within a D_{3h} geometry) is probed. The possibility of pentuple bonding in the latter system is explored. Different pathways for interconnecting stable conformations of the hydrides have been studied. These include separate considerations of rotating the bridging hydrides vs. rotation of one terminal ML_n group in $H_3M_2L_6$ and $H_4M_2L_8$ complexes. A coupled pseudorotation-rotation itinerary for $H_2M_2L_8$ is also examined.

Many transition-metal dimers and clusters have bridging ligands, most commonly carbonyls and halides.[2a-h] Perhaps less common, but no less interesting, is the bridging hydride.[2i] In this work, part of a general study of the bonding, structure, and dynamics of transition-metal dimers and clusters,[3] we shall study theoretically the geometrical characteristics of a number of unsupported dimers and their hydrido-bridged structural relatives.

There are relatively few known complexes in which the number of bridging hydrides is more than one.[4] They have the general formulas $H_2M_2L_8$,[5,6] $H_3M_2L_6$,[7-10] and $H_4M_2L_8$.[11] The geometries for these dimers are shown in **1-3.** In these

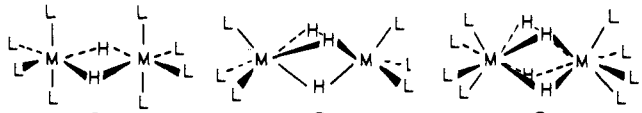

1 **2** **3**

three types of complexes the terminal ligands, L, are in an eclipsed arrangement relative to each other. The available evidence for the unsupported analogue of **1** is that conformation **4** is more stable. This is found for $Rh_2(PF_3)_8$[12] and has

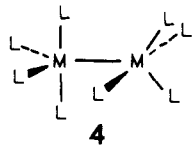

4

been suggested for the third isomer of $Co_2(CO)_8$.[13] The staggered, ethane-like conformation for unbridged M_2L_6 analogues of **2** is found for all d^3 dimers.[14] A number of other dimers with the M_2L_6 stoichiometry have been observed in matrix isolation[15] or ion cyclotron resonance[16] studies; however, details of their structure are not known. The unsupported M_2L_8 molecules of course include the classic case of the quadruply bonded $Re_2Cl_8^{2-}$ structures so elegantly studied by Cotton and co-workers. They are predominantly eclipsed,[17a,b] with two, so far isolated, nearly staggered variants.[17c]

The aim of the present paper is an understanding of the conformational preferences in these bridged systems and their unsupported analogues. Attention has been focused on two possible modes of internal rotation: (1) the rotation of the bridging hydrogen atoms and (2) the rotation of one group of terminal ligands. We have calculated the corresponding rotational barrier as a function of the number of d electrons of the metal atom M and as a function of the nature of the terminal ligand L (L = CO, H^-, Cl^-, i.e., respectively of π-acceptor, σ-donor, and π-donor character). Turning to systems not yet known, we have examined the possibility of bridging the metal-metal bond in M_2L_6 with five hydrides and in a D_{3d} M_2L_8 with three hydride ligands.

Our procedure is to derive the molecular orbitals of the unsupported dimers from the frontier orbitals of component ML_n fragments. The dimer orbitals are then interacted with the MOs of the bridging hydride grouping. The conclusions formed from such a fragment molecular orbital analysis[18] are supported by extended Hückel calculations. Computational details are specified in the Appendix.

M_2L_6 and $L_3MH_3ML_3$

As we have mentioned above, a number of d^3-d^3 M_2L_6 complexes have been prepared, and the structural and chemical

0002-7863/79/1501-3141$01.00/0

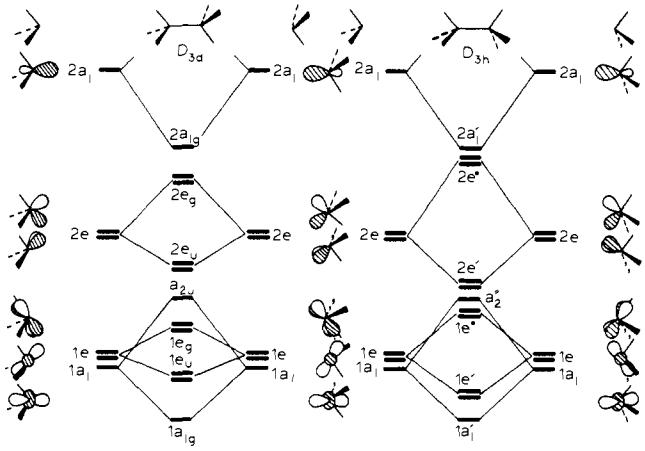

Figure 1. Interaction diagram for an M_2L_6 dimer in staggered (left) and eclipsed (right) conformations.

consequences of triple bonding in these molecules explored in detail by the Cotton and Chisholm groups.[14] All possess the D_{3d}, staggered, ethane-like geometry, **5**. The steric bulk of the

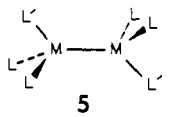

5

M = Cr, Mo, W

L = Me_2N, Et_2N, CH_2SiMe_3

L' = Cl, Me, Me_2N, Et_2N, CH_2SiMe_3

ligands may impose this conformation, for as we will show below the basic system should be eclipsed. Photoelectron spectra and X-α calculations on these compounds have been recently reported.[19]

To begin our discussion we bring together two ML_3 units in a D_{3d}, staggered, and a D_{3h}, eclipsed geometry. This is done in Figure 1. The familiar orbitals of the ML_3 fragment[20] are shown at extreme left and right. They consist of a low-lying $1a_1$ + 1e, remnants of the octahedral t_{2g} set, and a high-lying $2a_1$ + 2e. The e orbitals are "tilted", δ ($x^2 - y^2$, xy) and π(xz, yz) character (with respect to the M–M z axis to be formed) intermixed. The 1e set is primarily δ type, the 2e mainly π.

The a_1 levels of the ML_3 fragments are cylindrically symmetrical. So are the combinations formed from these in M_2L_6, which then do not contribute to a rotational barrier. Any conformational dependence arises from the e orbitals and their differential interaction in the eclipsed and staggered geometries.

Figure 1 shows clearly that the splitting between the e_g–e_u (e''–e') orbitals arising from interaction of fragment 1e and 2e orbitals is greater in the eclipsed form than in the staggered one. This is a result of the tilting, which creates a cylindrical asymmetry. There is greater overlap between the fragment e orbitals in the eclipsed geometry. The consequences on the rotational barrier of this will depend on the d electron count, as we well see.

The ordering of the M_2L_6 e levels is interesting, in that e_u orbitals emerge below e_g and e' below e''. This is also a consequence of the π–δ admixture. The two components of the $1e_u$, for instance, are shown in **6** and **7**. They are both δ antibonding

6

7

and π bonding. The converse is true for $1e_g$. Since the overlap of orbitals leading to a π bond is considerably stronger than that in a δ bond, the π character dominates, which leads to $1e_u$ lying below $1e_g$. The same is true for the 2e levels where the π character is supplied more by x, y than xz, yz. By a similar argument in the eclipsed geometry 1e' is δ and π bonding, 1e'' δ and π antibonding.

In a d^3–d^3 dimer, such as those known, the $1e_u$ or the 1e' level is filled. Clearly, from Figure 1, a preference for the eclipsed geometry is indicated. We look forward to a test of this risky prediction when d^3–d^3 M_2L_6 complexes with smaller ligands are prepared. Unfortunately dimerization, etc., of these molecules may predominate.

Putting four more electrons into the system fills 1e''–$1e_g$. The conformational preference is reversed, since 1e'' is destabilized more than 1e' is stabilized. In a d^8 dimer 2e'–$2e_u$ is now the HOMO which again favors the eclipsed geometry. Finally, in a d^{10} system, all levels are filled and, therefore, when taken together they form a cylindrically symmetrical set. Only a very small barrier arises. The values obtained from our extended Hückel calculations are given in Table I.

Table I. Calculated Barriers of Rotation in M_2L_6 Complexes (kcal/mol)[a]

	L			overlap deletions[b]	
d^n	CO	H	Cl	H	Cl
d^0	0.2	0.5	0.4	0.2	0.5
d^3	−9.3	−11.0	−4.3	−9.3	−5.7
d^5	1.3	3.2	5.4	3.3	6.8
d^8	−0.7	−2.6	−3.6	−3.5	−4.6
d^{10}	0.05	0.1	0.1	0.0	0.1

[a] A positive barrier indicates that the staggered D_{3d} geometry is more stable than the eclipsed D_{3h} one. [b] All non-nearest-neighbor interactions were deleted. See text.

Although there have been many interpretations of the origin of the rotational barrier in ethane, most have singled out closed-shell interactions between the hydrogens or between the C–H bonds.[21] In our calculations deleting all non-nearest-neighbor interactions in ethane produces a very small barrier. However, as shown in Table I, when these interactions are neglected for the M_2L_6 series there is essentially no change in the magnitude of the barrier. This again reaffirms our contention that the barrier in these dimers (with relatively small ligands) is due to the tilting of the 1e and 2e orbitals of the ML_3 fragment.

Note that the interaction diagram in Figure 1 predicts that $Co_2(CO)_6$, a d^9 dimer recently observed by matrix isolation techniques,[15] would have two electrons in 2e'' (or $2e_g$) and, therefore, likely undergo a Jahn–Teller distortion to an alternative geometry. This need not be the case. If the Co–Co distance is particularly short $2a_1'$ ($2a_g$) can lie lower in energy and accept the two additional electrons. In that case we predict the D_{3h}, eclipsed geometry to be the more stable one.

We now turn our attention to the $H_3M_2L_6$ system. As we have indicated already, there are known complexes of this type, the solid-state structures of several having been determined.[7,9,10] The bridging hydrogens have been located in the $H_3Fe_2(P_3)_2^+$ molecule[9] (P_3 = $CH_3C(CH_2PPh_2)_3$) and in $H_3Co_2(As_3)_2^+$ [9](As_3 = $CH_3C(CH_2AsPh_2)_3$). These two possess the confacial bioctahedral geometry, **2**.

At this point, before we begin our detailed study, we must share with the reader a problem of nomenclature. For M_2L_6 the trivial descriptors staggered and eclipsed are adequate and useful labels. The $L_3MH_3ML_3$ system, on the other hand, presents at least three way points that are worth discussing along a rotation itinerary, **8a–c**. An unambiguous notation in terms of torsional angles could, of course, be devised, but it will not have mnemonic character. The words "staggered" and "eclipsed" by themselves are ambiguous in this instance. We will try to reserve those words for unambiguous cases and skirt these problems in general with a numbered structure notation

with which we will proceed to analyze the reasons for the observed conformational preference. In a separate paper we will

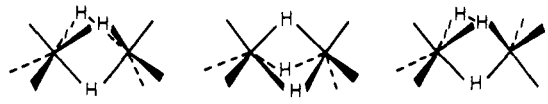

8a **8b** **8c**

examine a wider range of confacial bioctahedral systems $L_3MX_3ML_3$, with an emphasis on the role of monomer fragment geometry, through-bond coupling, and metal–metal binding as a function of the terminal and bridging ligands.[23]

The obvious construction of the hydride-bridged system is from the orbitals of M_2L_6 in Figure 1 and the three orbitals of a central H_3^{3-}, shown in **9.** Using the orbitals of the eclipsed

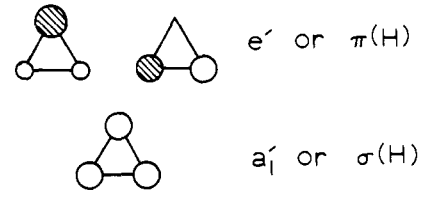

9

D_{3h} M_2L_6 we examine in Figure 2 two alternative geometries: **8a** (hydrogens staggered with respect to the metal ligands), the confacial bioctahedron at left, and **8b** (hydrogens eclipsed with respect to the metal ligands) at right.

The interaction of σ(H) with $1a_1'$ is equal in both orientations. On the other hand, the interactions of π(H) with 1e′ and 2e′ depend strongly on the orientation of the bridging fragment. In **8a** (left side of Figure 2) π(H) interacts mainly with 2e′ Since the 1e′ is mostly δ, and because of its tilting, π(H) has almost no overlap with 1e′, as shown in **10.** On the other hand, 2e′ is mainly π and the orbitals are tilted in such a manner as to give maximum overlap between the fragments. This is indicated in **11.** The relevant fragment overlaps (L = H) are

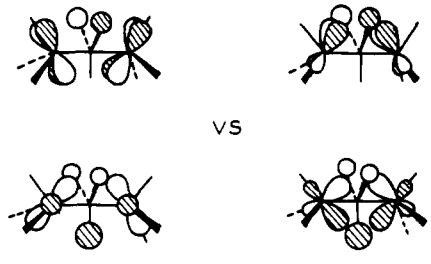

$\langle 1e'|\pi(H)\rangle = 0.067$ $\langle 2e'|\pi(H)\rangle = 0.360$

10 **11**

listed below the structures. Clearly the 2e′ interaction dominates.

The situation is quite different in the all-eclipsed conformation **8b.** Because of the tilting in the e′ sets of M_2L_6, the overlap between π(H) and 1e′ is now quite important whereas that between π(H) and 2e′ has lessened somewhat. This is shown in **12.** Conformation **8b** is therefore characterized (right

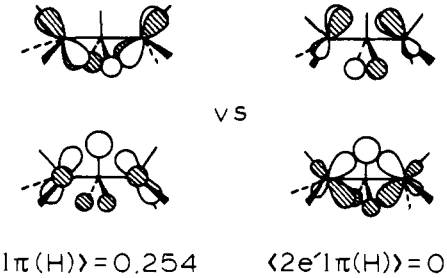

$\langle 1e'|\pi(H)\rangle = 0.254$ $\langle 2e'|\pi(H)\rangle = 0.254$

12

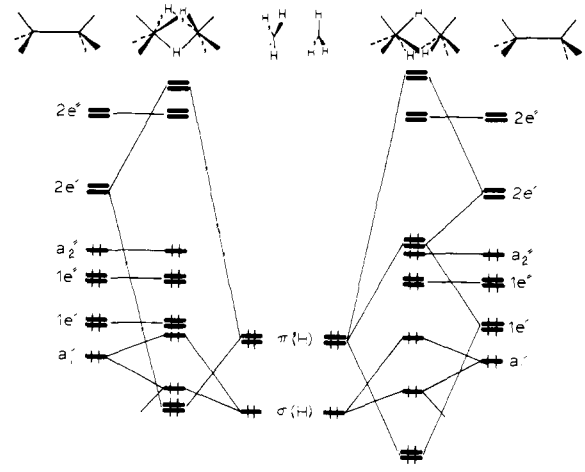

Figure 2. Interaction of the valence orbitals of eclipsed M_2L_6 with an H_3 fragment in conformations **8a** (left) and **8b** (right). The electron count shown is appropriate for $P_3FeH_3FeP_3^+$ or $(CO)_3ReH_3Re(CO)_3^-$

side of Figure 2) by a strong interaction between 1e′ and π(H), because of this large overlap, *and* also because of a good energy match. This four-electron destabilizing interaction is the key to the conformational preference for the other geometry, the confacial bioctahedral **8a.** (There is, however, a slight stabilization of the antibonding combination π(H)–1e′ by the empty set 2e′). Our extended Hückel calculations give a barrier of 45 kcal/mol for a d^6 metal and L = H^-. We computed a value of 47 kcal/mol for the $[H_3Fe_2(PH_3)_6]^+$ system, which is a more realistic model of the $H_3Fe_2(P_3)_2^+$ molecule.[9]

8a and **8b** probe the rotation of the hydride triangle against a rigid M_2L_6 frame. One can also think of beginning in the favored geometry **8a** and twisting one ML_3 group while keeping the H_3ML_3 unit fixed. The intermediate geometry, **8c,** has a staggered M_2L_6 frame and hydrogens staggered with respect to one ML_3, eclipsed with respect to the other. A detailed analysis, not presented here, shows that the interactions are in this geometry intermediate between **8a** and **8b.** In the calculations **8c** emerges 23 (L = H^-) or 25 kcal/mol (L = PH_3) less stable than **8a.** Thus it is easier to rotate one ML_3 group in these molecules than both synchronously, relative to a fixed H_3 frame.

There is another way of describing the conformational preferences of the M_2L_6 and $H_3M_2L_6$ dimers. The $2a_1$ and 2e sets of the ML_3 fragment in Figure 1, when taken together, are the equivalent of a set of three hybrid orbitals, **13,** which are directed toward the three missing sites which would complete an octahedron.[20] The lower $1a_1$ + 2e set concentrates electron

13 **14**

density over the ML_3 directions, i.e., completes a trigonal prism, as shown in **14.**[20,24]

Although the hybrids in **13** are "better formed", pointed more toward another ML_3 unit, those in **14** still have a considerable capacity for bonding with another fragment because of the tilting. In the d^3 M_2L_6 dimers each hybrid in **14** can be considered to have one electron, and the simplified bonding picture in **15** implies an eclipsed conformation. In the d^6 dimers

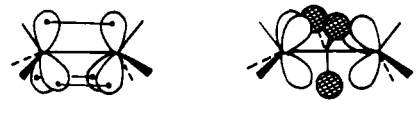

15 **16**

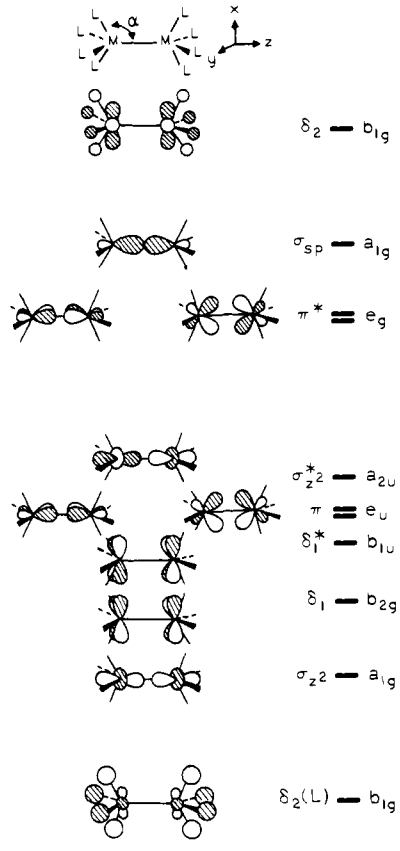

Figure 3. The important valence orbitals of D_{4h} M_2L_8.

each hybrid in **14** is doubly occupied. An eclipsed geometry would maximize four-electron repulsive interactions, and staggering is preferred. A d^9 system, such as $Co_2(CO)_6$ with a short Co–Co bond, will opt for the eclipsed geometry since there is now one electron in each of the hybrids **13.**

The $P_3FeH_3FeP_3^+$ dimer can be thought of as containing two Fe(II) centers, formally d^6, and three H^- bridging ligands. The three hybrids **13** are then empty. Their bonding combination ($a_1' + e'$) gives a set of orbitals ideally suited for reconstruction of the octahedron, **16,** by the hydrides. Maximum bonding is achieved only when the hydrides stagger with respect to the M_2L_6 core.

At this point it is appropriate to comment on the systems with two electrons more, e.g., $(As_3)CoH_3Co(As_3)^+$. Figure 2 shows that the two extra electrons enter the 2e″ orbital. A high-spin complex is expected, and the Co complex is indeed such.[9] The e″ orbital has by symmetry no H contribution, so the rotational preferences should be similar to the Fe dimer. But the 2e″ is metal–metal antibonding; for instance, one component of it is shown in **17.** One would anticipate a longer

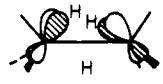

17

metal–metal bond in the Co complex than in the Fe. This is found: Fe–Fe 2.33 Å, Co–Co 2.38 Å.[9]

Calculated barriers for various d-electron configurations and terminal ligands are reported in Table II. In the d^0 and d^1 dimers conformations **8c** and **8b** are favored for L = CO or H by the strong stabilizing interaction between π(H) and 1e′. The constancy of the barriers on going from d^6 to d^8 has been discussed above.

Tables I and II show that variation in the electronic properties of L produces changes in the magnitude of the rotational barriers in M_2L_6 and $H_3M_2L_6$ compounds. One general feature is the ordering: π acceptor < σ donor < π donor. This trend is linked to the tilting of the e sets in the ML_3 fragments.[20a,23] The amount of tilting is in the order CO < H < Cl. If there would be no tilting in the ML_3 fragment orbitals, then their linear combinations would be purely δ and π. A tiny barrier would be obtained in the M_2L_6 dimers. This is in fact what happens if the L_3 set is replaced by the isolobal cyclopentadienyl ligand. As the tilting becomes greater there is more intermixing of δ and π which consequently gives rise to a larger barrier.

Table II. Calculated Barrier of Rotation (kcal/mol) for One Terminal ML_3 Group (Both Terminal Groups, in Parentheses) in $H_3M_2L_6$[a]

d^n	L = CO	L = H	L = Cl
d^0	−15 (−28)	−18 (−33)	2 (3)
d^1	−16 (−29)	−18 (−33)	6 (12)
d^3	−3 (−2)	−1 (3)	19 (43)
d^6	17 (32)	23 (45)	34 (64)
d^8	16 (32)	20 (45)	30 (64)

[a] A positive barrier indicates that bioctahedral geometry **8a** is more stable than **8c (8b).**

The argument for the $H_3M_2L_6$ dimers runs as follows. If L is a π acceptor like CO, not only does the 1e′ set in Figure 2 have more δ character and the 2e′ more π character, but also the energies of 1e′ and 2e′ are lowered.[23] One will then get a greater two-electron stabilizing interaction between π(H) and 2e′ ($\langle\pi(H)|2e'\rangle = 0.397$) in conformation **8a.** However, the four-electron destabilizing interaction between π(H) and 1e′ in conformation **8b** is now smaller, the overlap $\langle\pi(H)|1e'\rangle$ being smaller (0.230) and the antibonding combination π(H)–1e′ being now quite stabilized by the 2e′ empty set. This results in a smaller barrier for the rotation of the bridging hydrogens. If L is a π donor like Cl, the e sets of ML_3 are more tilted, i.e., the 1e′ set of M_2L_6 has greater π character and the 2e′ more δ character. Consequently, 1e′ now has a larger overlap with the π(H) set and this leads to some destabilization of conformation **8a.** The overriding factor for the d^6–d^8 dimers is the diminished stabilizing effect of 2e′ with π(H) in the conformation **8b.** We can also trace the fact that **8a** is more stable than **8b** for the d^0 and d^1 dimers to this loss of stabilization and to steric effects between the lone pairs on Cl and the bridging hydrides.

$L_4MH_4ML_4$

A major achievement in modern inorganic chemistry is the recognition and exploration of quadruple bonding in M_2L_8 systems by Cotton and co-workers.[1a,17a,25a,e] We shall not study thoroughly the electronic structure and the conformational preferences of the M_2L_8 system since many theoretical papers have been devoted to this system.[25] Moreover, the level ordering of the orbitals is strongly dependent on the chosen geometry (see below). The specific geometry of the fragment M_2L_8 in $H_4M_2L_8$ is also quite different from the geometry of the unsupported complexes M_2L_8.[11]

We do need the valence orbitals of the M_2L_8 fragment as a theoretical way point on the way to the hydride-bridged complex. These orbitals are shown in Figure 3 for the case of L a σ donor such as PH_3 or H^-, and in the geometry of $H_2P_2MMP_2H_2$ core in $H_8Re_2(PEt_2Ph)_4$.[11] σ_{z^2} is the bonding combination of metal z^2 orbitals[26]; δ_1 and δ_1* (of b_{2g} and b_{1u} symmetry, respectively, in the D_{4h} geometry of the fragment) are the bonding and antibonding combinations of metal xy. The π_{xz} and π_{yz} orbitals form a set of e_u symmetry. Together with π*, these are mainly comprised of metal xz and yz (somewhat hybridized by mixing metal x and y). σ_{sp} is the bonding combination of the metal sp hybrids.[20b] Figure 3 shows

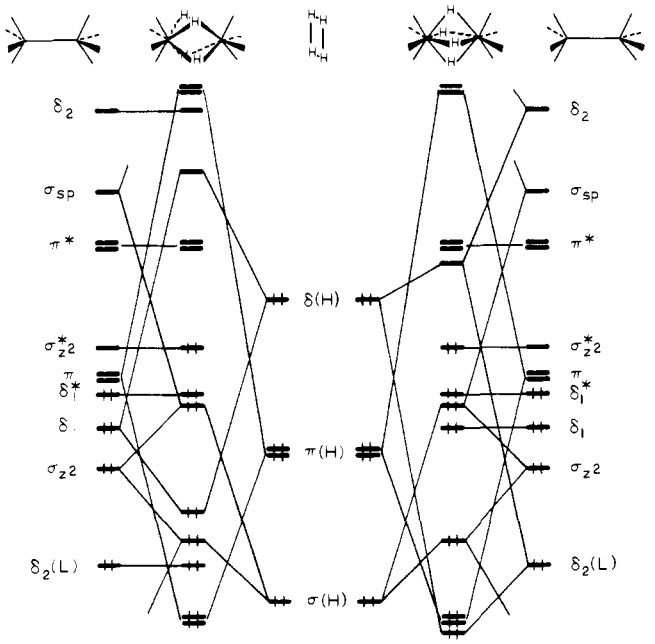

Figure 4. Interaction diagram for $H_4M_2L_8$ in conformations **19a** (left) and **19b** (right). The electron count is appropriate to $H_2P_2ReH_4ReH_2P_2$.

two other levels, one below and the other above the set of orbitals previously discussed. Both are of b_{1g} symmetry and will play a dominant role in setting the barrier for rotating the bridging hydrogens. The one at high energy, δ_2, is mainly the bonding combination of metal $x^2 - y^2$; the one at low energy, $\delta_{2(L)}$, is predominantly of ligand character with a small amount of metal $x^2 - y^2$.

The ordering $\sigma < \delta_1 < \delta_1^* < \pi$ in Figure 3 deserves some comment. The usual ordering is $\sigma < \pi < \delta_1 < \delta_1^*$ found, for instance, in the M_2Cl_8 dimers.[25] Going from M_2L_8 where L is a σ donor to M_2Cl_8 where Cl is a π donor will raise the energy of δ_1 and δ_1^* through antibonding between metal xy orbitals and Cl p orbitals. This is shown in **18** for δ_1. Moreover,

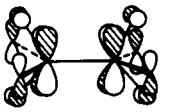

18

in the $H_4M_2L_8$ system and consequently in the M_2L_8 fragment, the ML_4 entity is more pyramidal than that in the M_2Cl_8 and related dimers. The M–M–L angle, α, shown at the top of Figure 3 was chosen to be 115.8°, the mean value in $H_8Re_2(PEt_2Ph)_4$.[11] A typical value of this angle in the M_2L_8 compounds is 105°.[17] Increasing the pyramidality of the ML_4 group will raise the energy of xz and yz since antibonding between the donor σ orbitals and metal orbitals is increased.[20b] Consequently the energy of both π and π^* in the M_2L_8 fragment will increase. Both of these trends produce the ordering of levels in Figure 3.

Three geometries are considered first, **19a–c.** Others were

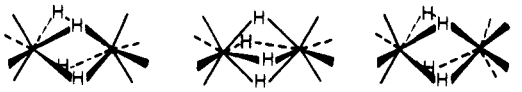

19a **19b** **19c**

also calculated, as will be discussed below. The eclipsed M_2L_8 fragment orbitals are of use in discussing the first two of these, through the interaction diagram of Figure 4. The M_2L_8 orbitals are at left and right, the four cyclobutadienoid H_4^{4-} combinations in the middle. The latter are shown separately in **20,**

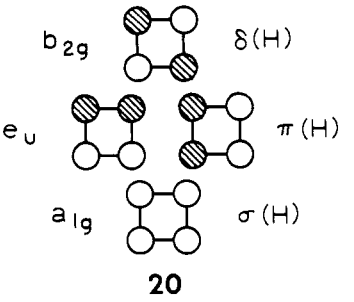

20

in a view along the MM axis. In both conformations studied in this figure there is some interaction between the σ(H) orbital of H_4^{4-} and the σ_{z^2} orbital (and to a lesser extent with the σ_{sp} orbital) of M_2L_8. There is a strong stabilizing interaction between the π(H) orbitals and the π orbitals of M_2L_8. Finally the interaction between δ(H) and the δ orbitals of M_2L_8 of appropriate symmetry for each conformation is stabilizing as well, since the corresponding antibonding combination is empty and the $\sigma^*_{z^2}$ level is occupied instead. In summary, the stability of the system results from the stabilization of π- and δ-like orbitals. A similar derivation of the bonding has recently appeared.[25j] Incidentally one will notice in Figure 4 that, since the π levels are now well below the δ_1 levels, the question of the ordering $\pi < \delta_1$ in M_2L_8 is irrelevant to the $H_4M_2L_8$ system.

The σ and π levels are both cylindrically symmetric and do not engender any conformational preference. The reason this occurs for the π levels is that a linear combination of the π(H) set, **21,** has precisely the same overlap with π in the geometry **19b** as the e_u combination shown in **20,** does for the confor-

21

mation **19a.** The rotational barrier will therefore arise from interactions between orbitals of δ symmetry. These are shown in **22** for the case where the hydrogens are staggered with respect to the terminal ligands, and in **23a** and **23b** for hydrogens

22

$\langle \delta(H) | \delta_1 \rangle = 0.293$

23a

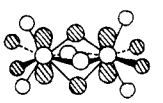

$\langle \delta(H) | \delta_2 \rangle = 0.148$

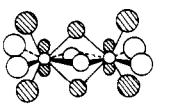

23b

$\langle \delta(H) | \delta_2(L) \rangle = 0.253$

eclipsing the ligands. Below the drawings are the corresponding overlaps, for L = H. Owing to a greater overlap and a better energy match (see Figure 4) the stabilization for $\delta_1 + \delta$(H) in the staggered conformation (**22, 19a**) is larger than the stabilization for δ_2(L) + δ(H) in the eclipsed (**23b, 19b**) conformation. For a metal with a d^3 configuration (Re^{IV}) the levels are occupied through the σ^*. **19a** is therefore more stable than **19b,** which agrees with the observed structure. Our extended Hückel calculations yield an energy difference between **19a** and **19b** of 44 kcal/mol for $H_4Re_2H_8^{4-}$ and 35 kcal/mol for $H_8Re_2(PH_3)_4$. In the latter molecule we calculate a tiny energy difference between the two conformations analogous to **19a** where the phosphines are cis and trans to one another.

An obvious alternative process consists of rotation of a single ML_4 group, leading to **19c.** This does not change the σ and π levels. But in a D_{3d} geometry of the M_2L_8 core the δ levels

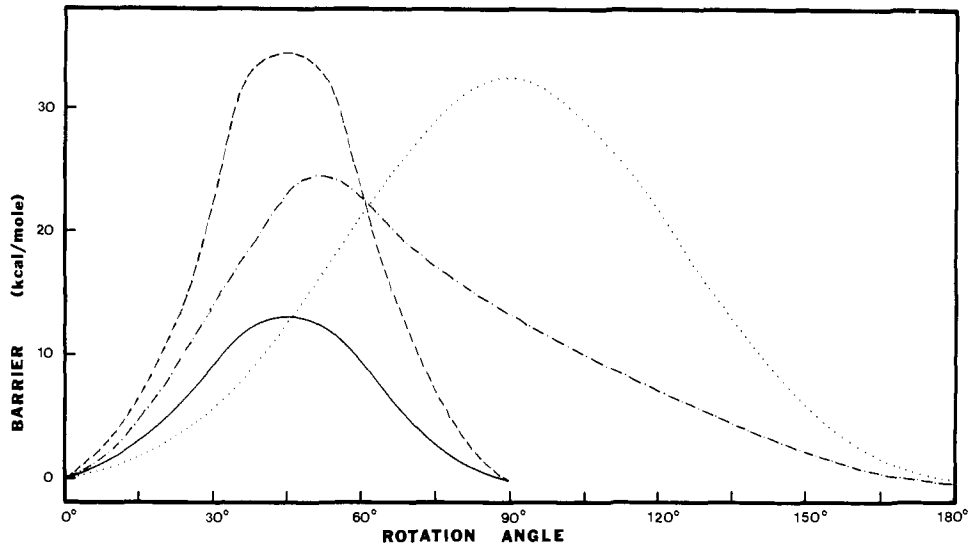

Figure 5. Barriers of rotation (kcal/mol) for $H_8Re_2(PH_3)_4$. The rotational processes in this figure correspond to: —, rotation of the terminal group only; - - - -, rotation of the bridging hydrogens only; • • • •, terminal group rotating twice as fast as the bridging hydrogens; - • - • - •, bridging hydrogens rotating twice as fast as the terminal group.

became a degenerate pair. Instead of δ_1 and δ_1* we have δ_a (**24**) and δ_b (**25**). They are pure metal xy or $x^2 - y^2$. δ_2 and δ_2* are transformed into $\delta_a^{\pm}$ (**26**) and $\delta_b^{\pm}$ (**27**), metal xy or $x^2 - y^2$

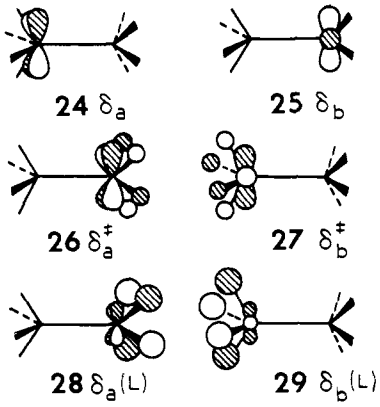

mixed in an antibonding way with σ donor orbitals. δ_a(L) (**28**) and δ_b(L) (**29**) are the bonding counterparts of these. In conformation **19c** the δ(H) orbital will overlap with δ_a, $\delta_a^{\pm}$, and δ_a(L), i.e., the orbitals which are xy-like. Since the overlaps are smaller than in the eclipsed or staggered conformation ($\langle\delta_a|\delta(H)\rangle = 0.201$, $\langle\delta_a^{\pm}|\delta(H)\rangle = 0.102$, $\langle\delta_a(L)|\delta(H)\rangle = 0.188$), the corresponding interactions will be smaller too and the whole system is not as strongly stabilized as in the conformation **19a,** but more so than in geometry **19b.** The rotation of one terminal group is therefore easier than rotating the bridging hydrogens. The extended Hückel values for the barrier were 15 kcal/mol for $H_4Re_2H_8^{4-}$ and 13 kcal/mol for $H_8Re_2(PH_3)_4$.

One could of course have imagined other modes of rotation, for instance, both the bridging hydrogens and the terminal group rotating at different speeds. We have computed two such paths for the $H_8Re_2(PH_3)_4$ system, one with the terminal group rotating twice as fast as the bridging hydrogens, the other with the bridging hydrogens rotating twice as fast as the terminal group. They are shown in Figure 5 together with the energy curves corresponding to the previously analyzed modes of rotation. One can easily see that rotation of a single terminal group is the most facile process, whereas rotation of the bridging hydrogens, which is of course identical with the simultaneous rotation of both ML_4 groups, is the most difficult one. It should be noted here that we have not yet considered any mechanisms for interconverting bridging and terminal hydrides, which is known to be a facile process in the Re hydride studied by Bau and co-workers.[11]

Table III. Calculated Barrier to Rotation[a] (kcal/mol) for One Terminal Group (Both Terminal Groups, in Parentheses) in $H_4M_2L_8$

d^n	L		
	CO	H	Cl
d^0–d^1	11 (13)	24 (44)	32 (77)
d^2–d^5	6 (13)	15 (44)	26 (77)

[a] A positive barrier indicates that **19a** is more stable than **19c** (**19b**).

Figure 4 also shows that the $H_4M_2L_8$ system may be stable in the staggered conformation for a metal with a configuration up to d^5. Had the metal a d^6 configuration, then the antibonding combination between δ(H) and δ_1 would be occupied, leading to apparent overall destabilization of the system. In the all-eclipsed conformation **19b** the antibonding combination between δ(H) and δ_2(L) would be occupied too, but the corresponding level is stabilized by the interaction with the empty δ_2 orbital. As a result the eclipsed conformation **19b** is now more stable than the staggered **19a** by 75 kcal/mol. This stabilizing interaction is not very large from our calculations and the system is in our calculations still unstable by 45 kcal/mol with respect to the two fragments. The reader is cautioned that our method may not be very reliable in this regard, i.e., stabilization energies of a complex relative to its fragments may not correctly reflect the energetics of complex formation.

Table III repeats the rotational barriers as a function of d-electron count and ligand set. In the rotation of the bridging hydrogens the values for the d^0–d^5 metal configurations are constant since one has only to empty or fill levels which are unaffected by the rotation (namely, σ_{z^2}, δ_1*, and π*). The smaller barriers of rotating one terminal group for the d^2–d^5 dimers in Table III compared to that found for d^0–d^1 come from the fact that a d^2 dimer has the δ_1* level filled (see Figure 4) which is higher in energy than the δ_b nonbonding level, **25,** in conformation **19c.** The increase of the barriers in the order π acceptor < σ donor < π donor can be rationalized, but the argument is not given here.

D_{2h} or D_{2d} M_2L_8 and $H_2M_2L_8$

The ML_4 moieties of an M_2L_8 dimer need not retain a local square pyramidal geometry. An excursion along a Berry

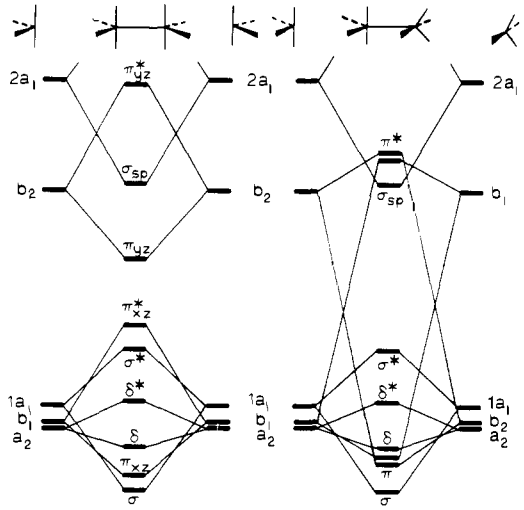

Figure 6. Interaction diagram for D_{2h} (left) and D_{2d} (right) M_2L_8.

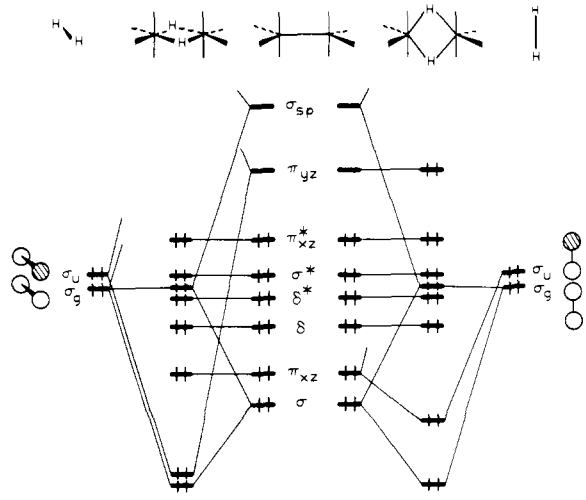

Figure 7. Interaction diagram for $H_2M_2L_8$ in conformations **32** (left) and **33** (right). The electron count shown is appropriate for $H_2W_2(CO)_8^{2-}$.

pseudorotation coordinate leads to a C_{2v} fragment, a piece of a trigonal bipyramid. Two such can combine to give geometrical extremes of D_{2d}, **30a**, and D_{2h}, **30b**, symmetry. As was

30a **30b**

mentioned in the introduction, a number of d^9 dimers, $Rh_2(PF_3)_8$,[12] $Ir_2(PF_3)_8$,[12] and one of the structural isomers of $Co_2(CO)_8$,[13,27] are found in the D_{2d} geometry.

The orbitals of a C_{2v} ML_4 fragment are well-known.[20b] They are shown in **31**. At low energy there is again a remnant

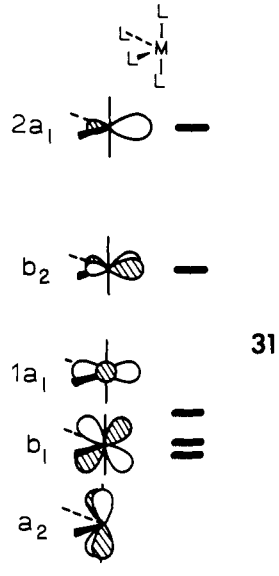

31

of the octahedral t_{2g}, a nest of three orbitals of a_2, b_1, and a_1 local symmetry. The a_2 and b_1 levels consist of metal xy and xz, respectively. When the equatorial L–M–L is 90°, $1a_1$ is a linear combination of z^2 and $x^2 - y^2$, giving a $z^2 - y^2$ orbital as shown in **31**. At higher energy is b_2. The equatorial ligand σ orbitals are antibonding with respect to metal yz, causing this level to lie at high energy. Furthermore, there is some mixing of metal y, in phase with respect to the ligand combination. This makes b_2 project away from L. Finally at still higher energy is $2a_1$, a hybrid of s,z and z^2.

Two such fragments are brought together to form the M_2L_8 dimer in D_{2d} and D_{2h} geometries in Figure 6. The dimer orbitals are labeled according to their σ, π, or δ pseudosymmetry.

The interactions are easily understood. Note that there is only one low-lying π bonding level in D_{2h}, π_{xz}, whereas in the D_{2d} form and in the undistorted D_{4h} there would be two. This is the result of the distortion from C_{4v} to C_{2v} in the ML_4 fragment. There are two known d^4 dimers[28] in which the normal D_{4h} geometry is distorted toward D_{2h}, but the metal–metal bond length in these is still indicative of a quadruple bond. The d^7 or d^8 dimers known at this time are comprised of square pyramidal units.[29-31] The interaction diagram of Figure 6 shows that the net bonding in the D_{2h} d^9 dimers is achieved through the bonding combination of the hybrid $2a_1$ orbitals.

The interconversion of the D_{2h} and D_{2d} geometries is a fascinating process, for it could involve a simple rotation around the metal–metal bond, a Berry pseudorotation at one or both metal centers, or a combination of these. We have not yet studied the complete surface for these motions. The rotation can be conveniently followed by a level correlation diagram. The σ and δ levels are relatively invariant to internal rotation. Therefore, large barriers are expected only when π-type levels are filled. In the d^9 dimers all π and π^* levels are occupied, and the expected and computed barrier is small (0.2 kcal/mol for L = CO, 0.3 for L = H, both favoring D_{2h}). For L = Cl the barrier is larger, favoring the D_{2d} geometry. This is an effect of a repulsive ligand–ligand interaction in the D_{2h} geometry, a steric effect. It is likely that the observed structures[12,13] also are a reflection of an optimization of steric factors.[27c]

The $H_2M_2L_8$ system has also been discussed in some detail by other workers.[32,33] Most of the bonding arises from interaction of the σ_g and σ_u orbitals of H_2^{2-} with the σ_{sp} and π_{yz} orbitals of M_2L_8. This is shown on the left side of the interaction diagram in Figure 7 and corresponds to the conformation observed for $H_2W_2(CO)_8^{2-}$ [6] and $H_2Re_2(CO)_8$.[5] The electron counting in Figure 7 is that for a d^6 dimer. Recall that σ_{sp} and π_{yz} originate from $2a_1$ and b_2 of ML_4 which in turn can be derived from the two equivalent orbitals pointing toward the missing ligand sides of an octahedral ML_6 system.[20b] Thus the octahedral environment of the metals has been recreated in $H_2M_2L_8$. This also explains why one should expect a large barrier in going from the "octahedral" geometry of **32** to that in **33**.

32 **33**

In terms of orbital interactions one has replaced the very strong stabilizing interaction of π_{yz} with σ_u, shown in **34** with

34 35

a weaker one between π_{xz} and σ_u, **35**.[34] This overlap difference is again linked in a transparent manner to the hybridization inherent in π_{yz}.

The calculated barrier between **32** and **33** for a d^6-d^6 dimer is 125 kcal/mol for L = H^- and 103 kcal/mol for L = CO. For a d^5-d^5 system, which is not known for bridging hydride, but is available for other bridging groups,[32] the barrier is somewhat lower but still high.

A possible alternative pathway for intramolecular hydrogen exchange in $H_2M_2L_8$ involves pseudorotation of the ML_4 units coupled with H_2 rotation, through a transition state **36**. It turns

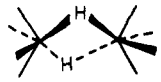

36

out to be of somewhat lower energy in the d^5 system, but not in d^6.

Hypothetical $H_5M_2L_6$

We have examples of up to four hydrides bridging two metal centers. Could one have five? The constraint is probably more steric than electronic, as we shall see.

The main problem is to combine H···H nonbonding contacts together with M-H bonding distances. The shortest intramolecular H···H contact distance is probably around 1.85 Å and a reasonable M-H bonding distance would be of the order of 1.9 Å,[9,11] an upper limit being perhaps 2.1 Å. Another geometrical constraint is the M-M bonding distance, which cannot be much less than 2.1 Å.[35] With these limits one gets a rather narrow range of likely geometries for $H_5M_2L_6$ candidates. We have chosen a M-M distance of 2.5 Å and an M-H distance of 1.9 Å. The resulting H · · · H distance then becomes 2.04 Å.

Which M_2L_n system would be a good candidate in order to bridge the metal-metal bond by five hydrogen atoms? Taking into account the analogy of such $H_5M_2L_n$ systems, with the triple decker sandwich compounds which have been previously discussed,[39] we chose to investigate the stability of $H_5M_2L_6$, **37**. With either L = CO or L_3 = Cp^- [40] the main difference

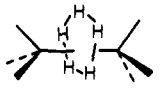

37

between $H_5M_2L_6$ and the triple decker sandwich compounds is that the middle ring in $H_5M_2L_6$ does not have orbitals of e″ symmetry but only orbitals of e′ symmetry to interact with the orbitals of M_2L_6.

The five orbitals of a H_5^{5-} ring are shown in **38** and their

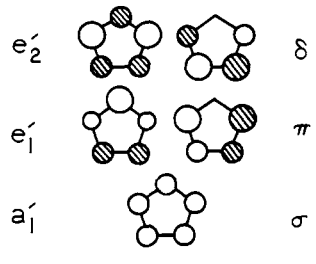

38

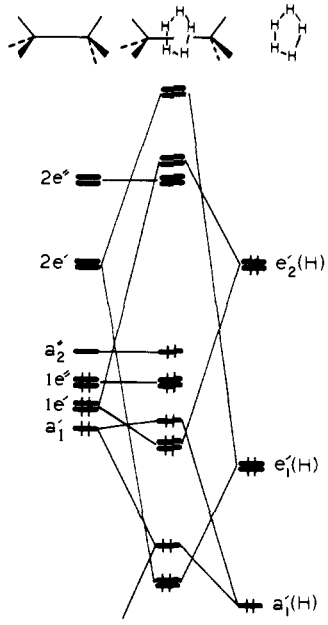

Figure 8. Construction of the orbitals of $H_5M_2L_6$.

interaction with M_2L_6 in Figure 8. Both $e_1'(H)$ and $e_2'(H)$ find a strong bonding interaction with 2e′ and 1e′ of M_2L_6, respectively. For a d^4 dimer, as shown in Figure 8, the orbitals are filled through the nonbonding $1a_2''$ of M_2L_6. The $H_5M_2L_6$ system is stabilized by 9.4 and 12.4 eV for $H_5Fe_2(PH_3)_6^{3+}$ and $H_5Fe_2(CO)_6^{3+}$, respectively, although the reader is cautioned that these numbers from extended Hückel calculations are not expected to be very reliable. The increase on going from a σ donor to π acceptor is easily rationalized. We previously showed that in $H_3M_2L_6$ the two-electron stabilizing interaction between π(H) and 2e′ is greater when L is a π acceptor. The same effect is operating here.

Although the interaction diagram in Figure 8 tells us that the $H_5M_2L_6$ system will be most stable for a metal with up to a d^4 configuration, a d^6 dimer may also be stable. For such a system we computed stabilization energies of 3.0 and 4.1 eV for L = PH_3 and CO, respectively. In conclusion, there is no a priori electronic reason that a $H_5M_2L_6$ complex cannot exist. However, its existence may be precluded by steric demands. The 15-fold rotational barriers in these systems should be very small.

D_{3d} M_2L_8 and $H_3M_2L_8$. Pentuple Bonding?

There exist a number of M_2L_8 complexes which have the D_{3d} geometry **39**,[13,27a,42-44] rather than D_{3h}, **40**. Not unexpectedly, we find that the reasons for this are steric.

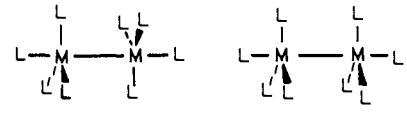

39 D_{3d} 40 D_{3h}

The important valence orbitals of the C_{3v} ML_4 fragment, shown on either side of Figure 9, partition themselves into two e sets and an a_1 orbital.[20b] The lower energy **1e** set consists of metal xz and yz and will form the π bond in the dimer. The 2e orbitals are comprised of metal $x^2 - y^2$ and xy and are destabilized by the ligand σ levels. As in the ML_3 fragment metal x and y are mixed into these levels to reduce this antibonding. Finally, the a_1 level is greatly destabilized by the ligand σ orbitals, in comparison to ML_3.

The D_{3d} M_2L_8 orbitals in the middle of Figure 9 are formed in a transparent manner, and are quite closely related to those

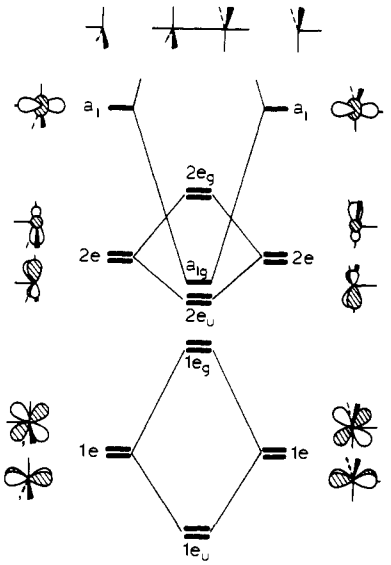

Figure 9. The orbitals of D_{3d} M_2L_8 constructed from two ML_4 fragments. The level occupation shown is for a d^4 dimer.

of a D_{3d} M_2L_6 geometry. In fact it would be easy to construct Figure 9 by approaching two axial ligands to the D_{3d} M_2L_6. The e_u level of M_2L_8, **41,** lies lower in energy than $2e_g$. This is again due to the greater π overlap between metal x, y compared to the δ overlap.

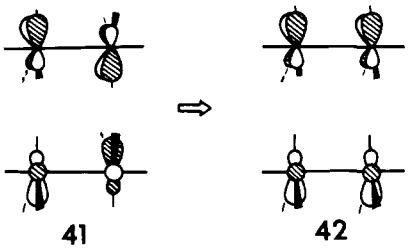

41 **42**

Upon rotation to the D_{3h} geometry the 2e′ set, **42,** which is both π and δ bonding, is now the more stable combination. Therefore, the 2e set is split to a larger extent in the D_{3h} conformation. The relationship of this behavior to that of 1e in the M_2L_6 dimers is obvious. There is little tilting (intermixing of $x^2 - y^2$ with yz and xy with xz) in the C_{3v} ML_4 fragment and, therefore, neglecting non-nearest-neighbor interactions, the 1e sets are split to an approximately equal extent in the D_{3d} and D_{3h} conformations of the dimer. Steric repulsions between ligands in **40** are severe, leading to a relatively large preference for the D_{3d} geometry, **39,** in d^0–d^{10} dimers when L = CO or Cl. A d^6 or d^7 dimer for the smaller hydride ligand is calculated to be more stable in the D_{3h} geometry by 5.4 kcal/mol because of the difference indicated by **41** and **42.** The D_{3d} geometry is slightly more stable (0.4–2.9 kcal/mol) for the other electronic configurations.

When L is a strong π but a relatively weak σ donor, like Cl^-, the energy gap between 1e and 2e of the C_{3v} ML_4 group is diminished. Consequently $1e_g$ in Figure 9 will lie close to the $2e_u$ and a_{1g} levels. Pushing this tendency still further, one might speculate if it is possible to make the $2e_u$ and a_{1g} levels lie below $1e_g$ or, better still, in the D_{3h} geometry to push 2e′, **42,** and a′ below 1e″ (the counterpart of $1e_g$). Were this possible *a d^5 dimer would have a formal bond order of five.* The existence of such a pentuple bond will be favored in the D_{3h} geometry since the 2e levels are split to a greater extent in this combination. A possible candidate, **43,** maintains the D_{3h} conformation through the use of bidentate bridging ligands. It would also be preferable to use bridging ligands that are poor σ donors, while at the same time having strong π donor functions

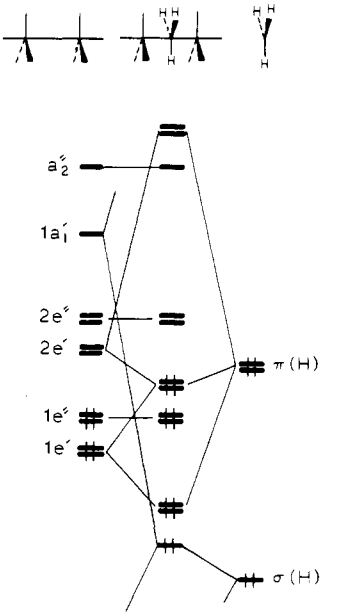

Figure 10. Interaction diagram for $H_3M_2L_8$ in conformation **44.** The electron count shown is for a d^4 dimer.

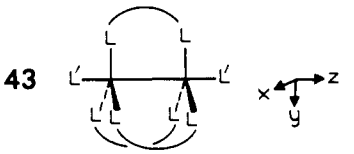

aligned along the L′–M–M–L′ axis. The latter would serve to destabilize the 1e combinations (metal xz and yz) while keeping the energy of the 2e combinations relatively low.

As in the case of $H_5M_2L_6$, the existence of $H_3M_2L_8$ complexes may also be precluded by steric interactions. For instance, in the hypothetical $H_3Fe_2(CO)_8$ system with a metal–metal bond length of 3.0 Å and a nonbonding H···H contact of 2.0 Å (this gives a value of 1.893 Å for the Fe–H distance), the nonbonding C_{eq}···H distance has a value of 2.167 Å in the staggered conformation **44.** Such a short distance is still possible. However, this distance would have a value of 1.625 Å in the eclipsed conformation **45.** If such a compound

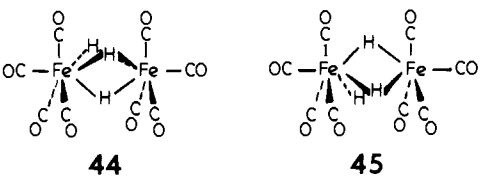

44 **45**

exists, its conformational preferences will be governed by steric interactions only and the possibility of an eclipsed conformation, **45,** would be excluded.

The interaction diagram for $H_3M_2L_8$ is shown in Figure 10. The 1e′–1e″ and 2e′–2e″ energy differences are much smaller in this figure than those shown in Figure 9. This is a reflection of the longer M–M bond length in the M_2L_8 fragment that we have chosen so as to minimize close contacts in the hydride. The 1e′ and 1e″ levels correspond to $1e_u$ and $1e_g$, respectively, in Figure 9. 2e′ is shown in **42** and 2e″ is its antibonding counterpart. The reader is referred back to **9** for the fragment orbitals of the bridging hydride triad. For a M_2L_8 fragment with a metal d^4 configuration the 1e′ and 1e″ sets of M_2L_8 are occupied. The major interaction is between 1e′ of M_2L_8 and π(H) of the hydride triad. This interaction is in principle destabilizing since both sets are occupied. However, the antibonding combination of 1e′ with π(H) is stabilized by 2e′. This mixing, indicated for one component of the e set in **46,** stabilizes the

Table IV. Parameters Used in Extended Hückel Calculations

orbital		H_{ii}, eV	ζ_1[a]	ζ_2[a]
Fe	4s	−9.10	1.9	
	4p	−5.32	1.9	
	3d	−12.6	5.35 (0.5505)	2.00 (0.6260)
W	6s	−8.26	2.341	
	6p	−5.17	2.309	
	5d	−10.37	4.982 (0.6940)	2.068 (0.5631)
Re	6s	−9.36	2.398	
	6p	−5.96	2.372	
	5d	−12.66	5.343 (0.6662)	2.277 (0.5910)
P	3s	−18.6	1.6	
	3p	−14.0	1.6	
Cl	3s	−26.3	2.033	
	3p	−14.2	2.033	
C	2s	−21.4	1.625	
	2p	−11.4	1.625	
O	2s	−32.3	2.275	
	2p	−14.8	2.275	
H	1s	−13.6	1.3	

[a] ζ is the Slater exponent whose coefficient of the double ζ expansion is given in parentheses.

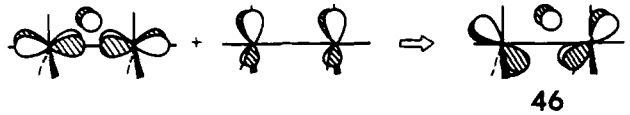

46

whole system with respect to the two fragments: 5.8 eV for $H_3Fe_2H_8^{3-}$ and 7.7 eV for $H_3Fe_2(CO)_8^{5+}$. While the magnitudes of these numbers are not expected to be reliable, we think that the trend is.

For a π donor ligand set such as Cl^- the system is destabilized. This is a steric effect. The Cl · · · H separations are 2.42 Å (with M-M 3.0 Å, M-H 1.893 Å), which is much smaller than the sum of the van der Waals radii. In fact, it is not possible to design a $H_3M_2Cl_6$ structure equivalent to **44** which has realistic M-H bond lengths and Cl-H nonbonding contacts.

Acknowledgments. We are grateful to Professor R. Bau for providing us structural information prior to publication. A.D. is grateful to the National Science Foundation and the Centre National de la Recherche Scientifique for making his stay at Cornell possible through an NSF-CNRS exchange award. The work at Cornell was generously supported by NSF Grant CHE 7606099 and that at Houston by the Robert A. Welch Foundation.

Appendix

All calculations were performed using the extended Hückel method.[45] The parameters used for Fe in the $H_3Fe_2L_6$, $H_3Fe_2L_8$, and $H_5Fe_2L_6$ systems were taken from earlier work.[3a] The H_{ii}'s for tungsten (in $H_2W_2L_8$) and rhenium (in $H_4Re_2L_8$) were obtained from charge iterative calculations on $H_2W_2(CO)_8^{2-}$ and $Re_2Cl_8^{2-}$ using the experimental geometries.[6,46] The values for the H_{ii}'s and orbital exponents are listed in Table IV. The modified Wolfsberg-Helmholz formula[47] was used throughout for these calculations. The experimental M-M bond lengths were chosen for the $H_3Fe_2L_6$,[9] $H_4Re_2L_8$,[11] and $H_2W_2L_8$[6] systems. The M-M bond length was set at 2.5 and 3.0 Å in the $H_5Fe_2L_6$ and $H_3Fe_2L_8$ complexes, respectively. The M-P(PH_3) distances were set to Fe, 2.22 Å, Re, 2.335 Å; the M-H (terminal) distances to Fe, 1.6 Å, Re, 1.669 Å,[11] W, 1.65 Å; the M-H (bridged) distance to Fe, 1.83 Å[9] in $H_3Fe_2L_6$, 2.043 Å in $H_5Re_2L_6$, 1.893 Å in $H_3Fe_2L_8$, Re, 1.879 Å,[11] W, 1.857 Å[6]; the M-C(O) distance to Fe, 1.78 Å, Re, 1.85 Å, W, 1.97 Å;[6] the M-Cl distance to Fe, 2.2 Å, Re, 2.33 Å, W, 2.48 Å. The L-M-L angles in the $H_nFe_2L_6$ systems were set at 90°, the M-M-L angles were set at 115.8° in all the $H_4Re_2L_8$ systems, but in the $H_8Re_2(PH_3)_4$ system the experimental[11] values were chosen (i.e., ∠Re-Re-H = 115.8°, ∠Re-Re-P = 128.6°), the W-W-L(ax) and W-W-L(eq) angles were idealized at 90 and 135°, respectively. The C-O and P-H distances were idealized at 1.14 and 1.42 Å, respectively. The M-M bond lengths in the unsupported dimers were idealized at 2.6 Å. The rest of the geometry was identical with that given above for the bridging hydride dimers.

References and Notes

(1) (a) Universite Louis Pasteur; (b) University of Houston; (c) Cornell University.
(2) For recent reviews of the structural and dynamic properties of these complexes, see (a) F. A. Cotton, *Prog. Inorg. Chem.*, **21**, 1 (1976); R. D. Adams and F. A. Cotton in "Dynamic Nuclear Magnetic Resonance Spectroscopy", L. M. Jackman and F. A. Cotton, Eds., Academic Press, New York, 1975, pp 489–522; (b) E. L. Muetterties, *Science*, **196**, 839 (1977); (c) R. Ugo, *Catal. Rev.-Sci. Eng.*, **11**, 225 (1975); (d) K. Wade, *Adv. Inorg. Chem. Radiochem.*, **18**, 1 (1976); (e) J. Evans, *Adv. Organomet. Chem.*, **16**, 319 (1977); (f) P. Chini, *Inorg. Chim. Rev.*, 31 (1968); (g) R. B. King, *Prog. Inorg. Chem.*, **15**, 287 (1972); (h) S. Aime and L. Milone, *Prog. Nucl. Magn. Reson. Spectrosc.*, **11**, 183 (1977). (i) For a review of hydrido transition metal clusters see H. D. Kaesz, *Chem. Br.*, **9**, 344 (1973).
(3) Previous studies by our group in this area are (a) R. H. Summerville and R. Hoffmann, *J. Am. Chem. Soc.*, **98**, 7240 (1976); (b) P. J. Hay, J. C. Thibeault, and R. Hoffmann, *ibid.*, **97**, 4884 (1975); (c) J. W. Lauher, M. Elian, R. H. Summerville, and R. Hoffmann, *ibid.*, **98**, 3219 (1976); (d) D. L. Thorn and R. Hoffmann, *Inorg. Chem.*, **17**, 126 (1978); (e) B. L. Barnett, C. Krüger, Y.-H. Tsay, R. H. Summerville, and R. Hoffmann, *Chem. Ber.*, **110**, 3900 (1977); (f) R. Hoffmann, B. E. R. Schilling, R. Bau, H. D. Kaesz, and D. M. P. Mingos, *J. Am. Chem. Soc.*, **100**, 6088 (1978); (g) A. Dedieu and R. Hoffmann, *ibid.*, **100**, 2074 (1978); (h) P. K. Mehrotra and R. Hoffmann, *Inorg. Chem.*, **17**, 2187 (1978); (i) T. A. Albright and R. Hoffmann, *J. Am. Chem. Soc.*, **100**, 7736 (1978).
(4) For references on singly bridged metal-metal bonded molecules see R. A. Love, H. B. Chin, T. F. Koetzle, S. W. Kirtley, B. R. Whittlesey, and R. Bau, *J. Am. Chem. Soc.*, **98**, 4491 (1976); M. R. Churchill, B. G. DeBoer, and F. J. Rotella, *Inorg. Chem.*, **15**, 1843 (1976).
(5) M. J. Bennett, W. A. G. Graham, J. K. Hayano, and W. L. Hutcheon, *J. Am. Chem. Soc.*, **94**, 6232 (1972).
(6) M. R. Churchill and S. W.-Y. Chang, *Inorg. Chem.*, **13**, 2413 (1974); M. R. Churchill, S. W.-Y. Chang, M. L. Berch, and A. Davison, *J. Chem. Soc., Chem. Commun.*, 691 (1973).
(7) A. P. Ginsberg and M. H. Hawkes, *J. Am. Chem. Soc.*, **90**, 5930 (1968).
(8) C. White, A. J. Oliver, and P. M. Maitlis, *J. Chem. Soc., Dalton Trans.*, 1901 (1973).
(9) P. Dapporto, S. Midollini, and L. Sacconi, *Inorg. Chem.*, **14**, 1643 (1975).
(10) R. H. Crabtree, H. Felkin, G. E. Morris, T. J. King, and J. A. Richards, *J. Organomet. Chem.*, **113**, C7 (1976); R. H. Crabtree, H. Felkin, and G. E. Morris, *ibid.*, **141**, 205 (1977).
(11) R. Bau, W. E. Carroll, R. G. Teller, and T. F. Koetzle, *J. Am. Chem. Soc.*, **99**, 3872 (1977).
(12) M. A. Bennett, R. N. Johnson, and T. W. Turney, *Inorg. Chem.*, **15**, 2939 (1976); W. S. Sheldrick, private communication, cited in this paper.
(13) R. J. Sweany and T. L. Brown, *Inorg. Chem.*, **16**, 415 (1977).
(14) (a) F. A. Cotton, B. R. Stults, J. M. Troup, M. H. Chisholm, and M. W. Extine, *J. Am. Chem. Soc.*, **97**, 1242, 5625 (1975); M. H. Chisholm, F. A. Cotton, M. W. Extine, and B. R. Stults, *ibid.*, **98**, 4477 (1976); M. H. Chisholm, F. A. Cotton, B. A. Frenz, W. W. Reichert, L. W. Shive, and B. R. Stults, *ibid.*, **98**, 4469 (1976); M. H. Chisholm, F. A. Cotton, M. W. Extine, M. Millar, and B. R. Stults, *ibid.*, **98**, 4486 (1976); M. H. Chisholm and M. W. Extine, *ibid.*, **98**, 6393 (1976); M. H. Chisholm, F. A. Cotton, M. W. Extine, M. Millar, and B. R. Stults, *Inorg. Chem.*, **15**, 2244 (1976); M. H. Chisholm, F. A. Cotton, M. W. Extine, and B. R. Stults, *ibid.*, **15**, 2252 (1976); M. H. Chisholm, F. A. Cotton, M. W. Extine, M. Millar, and B. R. Stults, *ibid.*, **16**, 320 (1977); M. H. Chisholm, F. A. Cotton, C. A. Murillo, and W. W. Reichert, *ibid.*, **16**, 1801 (1977); M. Akiyama, M. H. Chisholm, F. A. Cotton, M. W. Extine, and C. A. Murillo, *ibid.*, **16**, 2407 (1977); M. H. Chisholm, F. A. Cotton, M. W. Extine, and C. A. Murillo, *ibid.*, **17**, 2338 (1978). (b) F. Huq, W. Mowat, A. C. Skapski, and G. Wilkinson, *Chem. Commun.*, 1079 (1971).
(15) R. L. Sweany and T. L. Brown, *Inorg. Chem.*, **16**, 421 (1977).
(16) R. C. Dunbar, J. F. Ennever, and J. P. Fackler, Jr., *Inorg. Chem.*, **12**, 2734 (1973).
(17) (a) For a review see F. A. Cotton, *Chem. Soc. Rev.*, **4**, 27 (1975). (b) D. M. Collins, F. A. Cotton, S. Koch, M. Millar, and C. A. Murillo, *J. Am. Chem. Soc.*, **99**, 1259 (1977); F. A. Cotton, L. D. Gage, K. Mertis, L. W. Shive, and G. Wilkinson, *ibid.*, **98**, 6922 (1976); F. A. Cotton, J. M. Troup, and T. R. Webb, D. H. Williamson, and G. Wildinson, *ibid.*, **96**, 3824 (1974); F. A. Cotton, B. A. Frenz, J. R. Ebner, and R. A. Walton, *Inorg. Chem.*, **15**, 1630 (1976); F. A. Cotton and W. T. Hall, *ibid.*, **16**, 1867 (1977). (c) M. H. Chisholm, F. A. Cotton, M. W. Extine, and W. W. Reichert, *J. Am. Chem. Soc.*, **100**, 153 (1978); F. A. Cotton, G. G. Stanley, and R. A. Walton, *Inorg. Chem.*, **17**, 2099 (1978).
(18) R. Hoffmann, H. Fujimoto, J. R. Swenson, and C.-C. Wan, *J. Am. Chem. Soc.*, **95**, 7644 (1973); H. Fujimoto and R. Hoffmann, *J. Phys. Chem.*, **78**, 1167 (1974).
(19) F. A. Cotton, G. C. Stanley, B. J. Kalbacher, J. C. Green, E. Seddon, and M. H. Chisholm, *Proc. Natl. Acad. Sci. U.S.A.*, **74**, 3109 (1977).
(20) (a) T. A. Albright, P. Hofmann, and R. Hoffmann, *J. Am. Chem. Soc.*, **99**, 7546 (1977); (b) M. Elian and R. Hoffmann, *Inorg. Chem.*, **14**, 1058 (1975);

(c) M. Elian, M. M.-L. Chen, D. M. P. Mingos, and R. Hoffmann, *ibid.*, **15,** 1148 (1976); (d) L. E. Orgel, "An Introduction to Transition-Metal Chemistry", Wiley, New York, 1960, p 174.
(21) See, for example, P. W. Payne and L. C. Allen, "Modern Theoretical Chemistry", Vol. 4, H. F. Schaefer III, Ed., Plenum Press, New York, 1977.
(22) Also related to this conformation is $(\mu\text{-}H)_2Os_3(CO)_{10}$, in which the Os-Os bond is bridged by two hydrogens and one $Os(CO)_4$ group. See M. R. Churchill, F. J. Hollander, and J. P. Hutchinson, *Inorg. Chem.*, **16,** 2697 (1977).
(23) R. H. Summerville and R. Hoffmann, to be published.
(24) There is a relationship between this hybridization and that discussed by L. Pauling, *Proc. Natl. Acad. Sci. U.S.A.*, **72,** 3799, 4200 (1975); **73,** 1403 (1976). See also R. Hultgren, *Phys. Rev.*, **40,** 891 (1932); V. E. McClure, Ph.D. Dissertation, University of California, San Diego, 1970.
(25) (a) F. A. Cotton and C. B. Harris, *Inorg. Chem.*, **6,** 924 (1967); (b) A. P. Mortola, J. W. Moskowitz, and N. Rösch, *Int. J. Quantum Chem., Symp.*, **8,** 161 (1974); (c) J. G. Norman Jr. and H. J. Kolari, *J. Chem. Soc., Chem. Commun.*, 303 (1974); J. G. Norman Jr. and H. J. Kolari, *J. Am. Chem. Soc.*, **97,** 33 (1975); **100,** 791 (1978); (d) M. Biagini Cinoli and E. Tondello, *Inorg. Chim. Acta*, **11,** L3 (1974); (e) F. A. Cotton and B. J. Kalbacher, *Inorg. Chem.*, **16,** 2386 (1977); F. A. Cotton and G. G. Stanley, *ibid.*, **16,** 2668 (1977); (f) M. Benard and A. Veillard, *Nouveau J. Chim.*, **1,** 97 (1977); M. Benard, *J. Am. Chem. Soc.*, **100,** 2354 (1978); (g) C. D. Gardner, I. H. Hillier, M. F. Guest, J. C. Green, and A. W. Coleman, *Chem. Phys. Lett.*, **41,** 91 (1976); M. F. Guest, I. H. Hillier, and C. D. Gardner, *ibid.*, **48,** 587 (1977); (h) M. D. Reingeverts and D. V. Korol'kov, *Teor. Eksp. Khim.*, **10,** 596 (1974); (i) P. J. Hay, *J. Am. Chem. Soc.*, **100,** 2897 (1978); (j) P. Brant and R. A. Walton, *Inorg. Chem.*, **17,** 2674 (1978).
(26) Throughout this paper we shall use the notation z^2, $x^2 - y^2$, xy, xz, yz for the n d orbitals and x, y, z for the $(n + 1)$ p.
(27) (a) For other work on $Co_2(CO)_8$ see G. Bor and K. Noack, *J. Organomet. Chem.*, **64,** 367 (1974); K. Noack, *Helv. Chim. Acta*, **47,** 1064, 1555 (1964); K. Noack, *Spectrochim. Acta*, **19,** 1925 (1963); G. Bor, *ibid.*, **19,** 2065 (1963). (b) $Rh_2(CO)_8$ and $Ir_2(CO)_8$ both show no evidence for a nonsupported structure at higher temperatures: L. A. Hamlan and G. A. Ozin, *J. Am. Chem. Soc.*, **96,** 6324 (1974). (c) D. L. Lichtenberger and T. L. Brown, *Inorg. Chem.*, **17,** 1381 (1978).
(28) (a) J. A. Potenza, R. J. Johnson, and J. San Filippo Jr., *Inorg. Chem.*, **15,** 2215 (1976); (b) W. K. Bratton and F. A. Cotton, *ibid.*, **8,** 1299 (1969).
(29) F. A. Cotton, B. G. DeBoer, M. D. LaPrade, J. R. Pipal, and D. A. Ucho, *Acta Crystallogr., Sect. B*, **27,** 1664 (1971).
(30) (a) K. R. Mann, J. G. Gordon II, and H. B. Gray, *J. Am. Chem. Soc.*, **97,** 3553 (1975); N. S. Lewis, K. R. Mann, J. G. Gordon II, and H. B. Gray, *ibid.*, **98,** 746 (1976); (b) A. L. Balch and M. M. Olmstead, *ibid.*, **98,** 2354 (1976); A. L. Balch, *ibid.*, **98,** 8049 (1976).
(31) J. P. Fackler, *Prog. Inorg. Chem.*, **21,** 55 (1976).
(32) B. K. Teo, M. B. Hall, R. F. Fenske, and L. F. Dahl, *J. Organomet. Chem.*, **70,** 413 (1974).
(33) R. Mason and D. M. P. Mingos, *J. Organomet. Chem.*, **50,** 53 (1973).
(34) The rotation from **32** to **33** (both of D_{2h} symmetry) is not orbitally forbidden since, in the C_2 symmetry of the molecule between these rotameric extremes, the levels of δ and π symmetry are allowed to mix.
(35) The shortest metal-metal bond known to date is the Cr-Cr quadruple bond in $Cr_2(2,6\text{-dimethoxyphenyl})_4$ (1.847 Å)[36a] and in $Cr_2(o\text{-}C_6H_4O)_4^{4-}$ (1.83 Å).[36b] All other known metal-metal bond lengths are greater than 1.96 Å.[14,17] The shortest Mo-Mo quadruple bond known has a length of 2.067 Å.[36] Typical values for Cr-Cr and Mo-Mo triple bonds are around 2.28[37] and 2.20 Å.[14] The bridged Cr-Cr bond in $Cr_2(CH_2SiMe_3)_4(PMe_3)_2$ has a length of 2.10 Å.[38]
(36) (a) F. A. Cotton, S. Koch, and M. Millar, *J. Am. Chem. Soc.*, **99,** 7373 (1977); (b) F. A. Cotton and S. Koch, *Inorg. Chem.*, **17,** 2021 (1978).
(37) J. Potenza, P. Giordano, D. Mastropaolo, and A. Efraty, *Inorg. Chem.*, **13,** 2540 (1974).
(38) R. A. Andersen, R. A. Jones, G. Wilkinson, M. B. Hursthouse, and K. M. Abdul Malik, *J. Chem. Soc., Chem. Commun.*, 283 (1977).
(39) J. W. Lauher, M. Elian, R. H. Summerville, and R. Hoffmann, *J. Am. Chem. Soc.*, **98,** 3219 (1976).
(40) The isolobal analogy[39] between the Cp and $M(CO)_3$ fragments makes the hypothetical system $H_3Fe_2(CO)_6^+$ very similar to the known compound $H_3Ir_2(C_5Me_5)^{+}$.[41]
(41) R. Bau, personal communication; R. Bau, W. E. Carroll, D. Hart, R. G. Teller, and T. F. Koetzle, *Adv. Chem. Ser.*, **No. 167,** 73 (1978).
(42) J. A. Ibers, *J. Organomet. Chem.*, **14,** 423 (1968).
(43) H. B. Chin, M. B. Smith, R. D. Wilson, and R. Bau, *J. Am. Chem. Soc.*, **96,** 5285 (1974).
(44) M. G. Newton, R. B. King, M. Chang, N. S. Pantaleo, and J. Gimeno, *J. Chem. Soc., Chem. Commun.*, 531 (1977).
(45) (a) R. Hoffmann, *J. Chem. Phys.*, **39,** 1397 (1963); R. Hoffmann and W. N. Lipscomb, *ibid.*, **36,** 3179 (1962); **37,** 2872 (1962).
(46) F. A. Cotton, B. A. Frenz, B. R. Stults, and T. R. Webb, *J. Am. Chem. Soc.*, **98,** 2768 (1976).
(47) J. H. Ammeter, H. B. Bürgi, J. C. Thibeault, and R. Hoffmann, *J. Am. Chem. Soc.*, **100,** 3686 (1978).

Luminescence Quenching of the Bis(2,2′-bipyridine)aquo-2,2′-bipyridineiridium(III) Ion and Its Conjugate Base

Steven F. Bergeron and Richard J. Watts*

Contribution from the Department of Chemistry, University of California, Santa Barbara, California 93106. *Received July 11, 1978*

Abstract: Quenching of $Ir(bpy)_2(H_2O)(bpy)^{3+}$ and $Ir(bpy)_2(OH)(bpy)^{2+}$ by a variety of charged metal complexes and neutral biacetyl has been studied. Stern-Volmer and quenching constants have been determined and diffusional rate constants for each donor-acceptor combination have been estimated. Quenching efficiencies are comparable to those of $Ru(bpy)_3^{2+}$ with similar quenchers. Quenching is believed to occur by both energy-transfer and electron-transfer mechanisms. The reduction potential of the luminescent state of $Ir(bpy)_2(OH)(bpy)^{2+}$ is estimated to be +1.84 V.

Introduction

Since the initial studies of the use of the tris(bipyridyl)-ruthenium(II) ion $[Ru(bpy)_3^{2+}]$ as a sensitizer,[1] there has been an enormous growth of interest in the use of this and other transition-metal ions to initiate photoinduced energy- and/or electron-transfer processes. Three broad areas of bimolecular photoinduced processes which have come under study are (1) quenching by oxidation electron transfer;[2-10] (2) quenching by reductive electron transfer;[11-16] (3) quenching by energy transfer.[17-23] A fourth photoinduced bimolecular process which has been reported for transition-metal complexes, though not widely studied, is excited-state proton transfer (4).[24,25]

$$*D^{n+} + A^{m+} \rightarrow D^{(n+1)+} + A^{(m-1)+} \quad (1)$$

$$*D^{n+} + A^{m+} \rightarrow D^{(n-1)+} + A^{(m+1)+} \quad (2)$$

$$*D^{n+} + A^{m+} \rightarrow D^{n+} + *A^{m+} \quad (3)$$

$$*D^{n+} + HX^{+} \rightleftarrows *HD^{(n+1)+} + X \quad (4)$$

The versatility of transition-metal complexes is illustrated by the fact that a single donor, such as $Ru(bpy)_3^{2+}$, may undergo all of the first three processes with appropriate selection of acceptors.

In a previous study[26] we reported the isolation of a stable complex of Ir(III) which contains bpy bound as a monodentate ligand, and noted that its photophysical properties (luminescence quantum yield, lifetime, emission energy) indicated that it might be useful as a high-energy sensitizer. Since then the complex $[Ir(bpy)_2H_2O(bpy)]^{3+}$ has been found to sensitize the norbornadiene to quadricyclene isomerization with high efficiency (~70% at 366 nm).[27] The conjugate base of this complex, $[Ir(bpy)_2OH(bpy)]^{2+}$, has photophysical properties similar to those of the acid, and also should be useful as a high-energy sensitizer. We report here the results of a study of the quenching of the emissions of the acid and base forms of this complex by a variety of acceptor species.

0002-7863/79/1501-3151$01.00/0